OPTICAL DIODES*

T. K. Gustafson

University of California, Berkeley

Since the previous laser energy conversion conference, significant progress has been made in understanding the rather detailed phenomena which have characterized optical diode work (See, for example, ref. 1.) Of particular interest to us has been the fact that such structures can couple and rectify infrared and optical radiation in complete analogy to similar structures operating at microwave or radio frequencies. A recent achievement has been a direct demonstration of antenna coupling and rectification characteristics with high resistance evaporated structures at a wavelength of 10 μ. Earlier, optically induced signals had been demonstrated at 6328 A. We feel that as a result of the 10-μ work that high frequency arrays are inevitable.

The present summary contains a descriptive review of some of the aspects of our own work on metal-barrier-metal structures. Coherent conversion of laser radiation and infrared and optical circuit elements are seen as among the potentially exciting applications of such devices. Figure 1 shows the two basic types of structures which we, as well as others, have utilized for these investigations. Although many of the results have been achieved with the point-contact type of diode structure, recent rapid development of the more stable photo-lithographic structures has also occurred. Some of the particular advantages and disadvantages of each are quite apparent:

Diode structure	Advantages	Disadvantages
Point-Contact	Low bulk loss Small area Clean antenna structure	Mechanical instability Etching problems
Evaporated (Photolithographic or electron beam)	Stability Ease of design Amenable to arrays and complex configurations	Large area Thermal problems Difficult to obtain low junction resistances

*Contributors: D. P. Siu, S. Y. Want, S. M. Faris, Tatzuo Izawa, R. Jain, and B. Fan, University of California, Berkeley.

In both the point contact and evaporated structures it is apparent that the primary mechanism involved is electronic tunneling. The appropriate band diagram is shown on the left-hand side of figure 2. The difference between the Fermi levels of the two metals is the applied voltage eV which upsets the dynamical equilibrium of electron exchange across the barrier. Simmons (ref. 2) has deduced the basic semi-classical expression given in figure 2. This is seen to depend exponentially upon the voltage. The characteristic thus displays curvature which can of course be used to rectify and therefore to convert electromagnetic energy to electrical energy.

S. M. Faris has performed extensive rectification experiments at 1.06 μ and 0.6328 μ, the results of which have been well explained by the rectification theory (ref. 3); that is, that the voltage difference eV between the Fermi levels is in fact the sum of the bias voltage plus an optically induced voltage whose frequency is that of the incident optical radiation. Since these results are published, it is sufficient for the present purposes to provide an outline of the theory and point out the important characteristics which are supported by the experimental observations. Figure 3 contains a summary of the steps in the derivation of the rectification signal in terms of the Bessel functions of an imaginary argument and figure 4 displays the comparison between experiment and theory for the rectification of the He-Ne 6328 Å radiation. Experimentally rectified voltage V_ω is obtained using phase sensitive detection (direct detection arrangement at a chopping frequency of 1 kHz) and is plotted as a function of a dc bias potential V_B. Comparing the experimental results with the theoretically predicted behavior, one notes the agreement in curvature and intersection with the $V_\omega = 0$ axis. This behavior depends upon the behavior of the Bessel functions of an imaginary argument and, because the parameter z is directly proportional to the barrier thickness, upon the impedance of the junction as well as the optical voltage.

By fitting the theoretical curves with those measured experimentally one is able to obtain an estimate of the optical voltage and coupling characteristics. One finds that the optical voltage is of the order of 100 mV. Assuming this to be induced across the junction through the whisker acting as an antenna, the effective area of the antenna must of the order of 4×10^{-8} cm^2. The coupling efficiency is found to be of the order of 10^{-5}, indicating the expected very poor mismatch.

The success of the rectification experiments has prompted further work in several important directions:

1. Basic experiments in which high frequency antenna coupling could be clearly demonstrated (ref. 4).

2. Basic experiments which would confirm tunneling predictions at high frequencies and the presence of negative differential resistance at high frequencies (ref. 5).

3. Design and demonstration of evaporated (photolithographically fabricated) junctions which would behave similarly to the point contact structure.

4. High frequency arrays which would couple more efficiently to a given laser mode.

Several experimental and theoretical considerations have already demonstrated the principles involved in several of these directions. At this point it is worthwhile considering these and indicating directions in which future effort is most likely to be concentrated.

Generalizing from the particular case of rectification, higher order mixing characteristics of the diode junctions can become considerably more complicated. Relating to the excitation and coupling, the nonlinear mixing can be current controlled rather than voltage controlled, the case considered thus far. In addition, since the quasi-static equations of Simmons describe the nonlinearity it is important to check the validity of theoretical predictions relating higher order mixing processes. Finally, with respect to potential conversion, one should ask whether rectification is the most appropriate process to exploit.

Experimental evidence thus far strongly suggests that the coupling and nonlinear mixing processes can be either voltage or current controlled depending upon the antenna and junction impedance, antenna loss, etc. (ref. 6). In the submillimeter and far-infrared portion of the spectrum current control appears to be almost exclusive.

Figure 5 shows a schematic of a general (n+1)th order mixing process involving two incident frequencies. This is the most common process involved and has been discussed earlier by several authors. For current excitation the RMS voltage at the i.f. frequency $V_n(\omega_1 - n\omega_2)$ is proportional to the (n+1)th derivative of the voltage with respect to the current as indicated in figure 5.

The theoretical results are shown for n = 1 to 6. The minima and maxima, which occur for finite bias voltages and which number n for (n+1)th order mixing are the most striking characteristic. These can be used to definitively distinguish current from voltage excitation. No such minima would occur for voltage controlled excitation.

These characteristics have been observed experimentally by Sakuma and Evensen (ref. 7). We have included one of their experimental results corresponding to n = 5 in figure 5 to illustrate the striking agreement. In addition to their experimental results, Javan has discussed oscillations in the detected signal and Faris has obtained experimental results at 1.15 μ for n = 1 (rectification) which indicate current controlled rectification. The latter is shown in figure 6.

We are presently investigating more general aspects of the mixing theory. In particular we are attempting to employ two diode structures, one as a transmitter and the other as a receiver, to investigate the characteristics directly at 10.6 μ. This would represent a generalization of the transmission-reception experiments carried out by Javan and others and has been discussed previously. The transmission diode is to be situated on one focus of a half-ellipsoidal cavity configuration and the receiving diode at the other focus. Heterdyne detection at this receiving diode is anticipated.

This experiment has provided a significant guide to the development of better diode structures and consideration of the coupling characteristics. Point contact structures are being replaced by more carefully designed, single junction, photolithographically fabricated structures; eventually arrays will be used. The successful achievement of such an experiment will require fairly sensitive structures whose coupling and junction characteristics are quite well known and designed.

With respect to the development of the photolithographically fabricated structures, significant progress has been made. Recent results are particularly encouraging and warrant optimism. Figure 7 displays the two dimensional single junction structures which are presently being utilized. On a germanium substrate, a nickel base plate is first fabricated. This is then oxidized to obtain an oxide layer $\simeq$ 15-Å thick. A gold antenna is then evaporated, the overlap with the nickel base forming the

metal-barrier-metal junction device. The current-voltage characteristic shown indicates that it is a tunneling junction of high quality with a zero bias resistance in the hundreds of kΩ range.

Figure 8 displays the detection characteristics of such a structure at 10.6 μ for a radiation intensity equal to 10 W/cm^2. The angle is measured between the normal to the substrate surface and the propagation vector of the incident laser beam. Parallel (") polarization represents the electric field polarized along the gold antenna and perpendicular, electric field polarization across the antenna.

For the high impedance structure " and $^{\perp}$'r polarization give very different results. The peak polarization ratio is $\simeq$ 20, parallel coupling being much larger at an angle of $\simeq$ 10° with respect to the substrate. Verification of the antenna coupling was accomplished by shortening the diode junction thereby preventing rectification. The "signal then behaves similarly to the $^{\perp}$'r signal both being characteristic of a cos θ thermally induced signal.

For such an antenna structure we have estimated the optical voltage to be 10^{-5} to 10^{-6} V for the 10 W/cm^2 incident intensity. The angular dependence of the detected signal for " polarization agrees well with that expected from antenna calculations.

We are presently extending these results to obtain resolution of the antenna lobes. We expect to work toward the ultraviolet portion of the spectrum where absorption becomes large and antenna coupling should fail. Figure 9 indicates several possible directions that are being considered. It is quite apparent that the micro-structures will become important as infrared and optical components, particularly in the light of the rapid development which has already occurred.

REFERENCES

1. Faris, S. M.; Gustafson, T. Kenneth; and Wiesner, John C.: Detection of Optical and Infrared Radiation with DC-Biased Electron-Tunneling Metal-Barrier-Metal Diodes. IEEE J. Q. E. Vol. QE-9, no. 7, July 1973, p. 737-745. Also see the preceding presentation by Ali Javan.

2. Simmons, John G.: Generalized Formula for the Electric Tunnel Effect Between Similar Electrodes Separated by a Thin Insulating Film. J. Appl. Phys. 34, no. 6, June 1963, 1793-1803. He has several other publications which appeared at this time in J. Appl. Phys; (for dissimilar electrodes see "Electric Tunnel Effect between Dissimilar Electrodes Separated by a "Thin Insulating Film." J. Appl. Phys. Vol. 34, no. 9 Sept. 1963, p. 2581-2590.

3. Does, J. W. "Detection and harmonic generation in the sub-millimeter wavelength region. Microwave J., Vol. 9, Sept. 1966, p. 48-55.

4. Previous mixing and detection experiments with clear indications of antenna coupling include: Matarrese, L. M.; and Evenson, K. M. "Improved Coupling to Infrared Whisker Diodes by Use of Antenna Theory." Appl. Phys. Lett. 17, no. 1, 1 July 1970, p. 8-10; Sanchez; A, Singh; S. K.; and Javan, A. Generation of Infrared Radiation in a Metal-to-Metal Point-Contact Diode at Synthesized Frequencies of Incident Fields: A High-speed Broadband Light Modulator. Appl. Phys. Lett. Vol. 21, no. 5, 1 Sept. 1972, p. 240-243; Radiation of Difference Frequencies Produced by Mixing in Metal-Barrier-Metal Diodes, p. 240-243 Gustafson, T. K; and Bridges, T. J.: Appl. Phys. Lett. Vol. 25, no. 1, 1 July 1974; p. 56-59; Recent Antenna Coupling Investigations of Point Diodes at 10.6 μm by Twu and Schwarz (private communication); and Small, J. G.; Elchinger, G. M.; Javan, A.; Sanchez, Antonio; Bachner, F. J.; and Symthe, D L.: AC Electron Tunneling at Infrared Frequencies: Thin-film M-O-M Diode Structure With Broad-band Characteristics. Appl. Phys. Lett. Vol. 24, no. 6, 15 March 1974, p. 275-279.

5. Negative differential resistance at low frequencies has been reported by Wang, S. Y.; Faris, S. M.; Siu, D. P.; Jain, R. K.; and Gustafson, T. K.: Enhanced Optical Frequency detection with Negative Differential Resistance in Metal-Barrier-Metal Point-Contact Diodes. Appl. Phys. Lett. Vol. 25, no. 9, 1 Nov. 1974, p. 493-495.

6. Farris, S. M.; and Gustafson, T. K.: Harmonic Mixing Characteristics of Metal-Barrier-Metal Junctions as Predicted by Electron Tunneling. Appl. Phys. Lett., Vol. 25, no. 10, 15 Nov. 1974, p. 544-549.

7. Sakuma, Eiichi; and Evenson, Kenneth M.: Characteristics of Tungsten-Nickel Point Contact Diodes Used as Laser Harmonic-Generator Mixers. IEEE J.Q.E., Vol. QE-10, no. 8, Aug. 1974, p. 599-603.

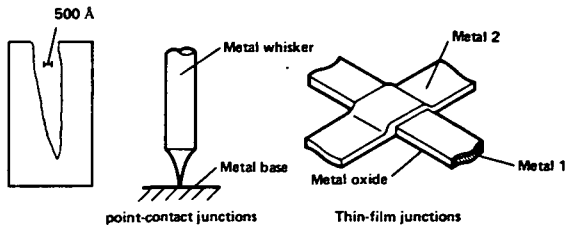

Figure 1.– Metal-barrier-metal structures. At the left is shown an electron microscope scan of an etched tungsten wire; point-contact geometry is shown in the center; and the early evaporated two-dimensional structure is at the right.

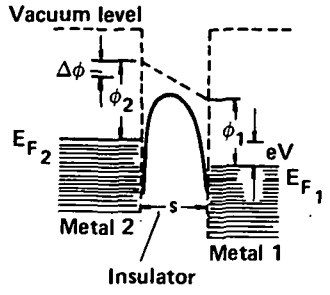

Potential barrier of M-B-M junction

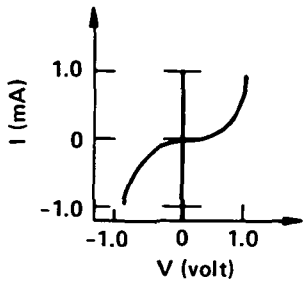

I-V characteristic of M-B-M junction

$$I(V) = \frac{e}{2\pi h(\Delta s)^2}\left\{ \bar{\phi}_f e^{-A_f\bar{\phi}_f^{1/2}} - (\bar{\phi}_f + eV)e^{-A_f(\bar{\phi}_f + eV)^{1/2}} \right\}, \quad V > 0$$

$$\bar{\phi}_f = \int_{s_1}^{s_2} \left[\phi_2 - (\Delta\phi + eV)\frac{x}{s} - \frac{\lambda s^2}{x(s-x)} \right] dx/\Delta s, \quad A_f \cong 1.025\,\Delta s$$

$\Delta s = s_2 - s_1$, s_1 , s_2 classical turning points

Figure 2.– Simplified band diagram and current-voltage characteristic of the metal-barrier-metal structure. The expression for I(V) is that deduced by Simmons. Parameter definitions are:

E_{F_1}, E_{F_2} Fermi energies of metals 1 and 2, respectively.

ϕ_1, ϕ_2 work functions of the two metals

$\Delta\phi = \phi_1 - \phi_2$

s barrier thickness

s_1, s_2 W.K.B. turning points for electrons with energy: E_{F_2}

$\Delta s = s_1 - s_2$

$eV = eV_B + ev(t)\cos\omega t$, where V_B is the voltage bias

f forward for which metal 2 is positive with respect to metal one. For opposite bias a similar expression is obtained as shown in figure 3.

v(t) the induced optical voltage and ω the optical frequency

λ parameter defining strength of surface charge ($\cong$ 5 Å(eV))

$$\left.\begin{aligned} I_f(V) &= J_f\left\{\bar{\phi}_f \exp(-A_f\bar{\phi}_f^{1/2}) - (\bar{\phi}_f + eV)\exp[-A_f(\bar{\phi}_f + eV)^{1/2}]\right\}; \quad V > 0 \\ I_r(V) &= J_r\left\{(\bar{\phi}_r - eV)\exp[-A_r(\bar{\phi}_r - eV)^{1/2}] - \bar{\phi}_r \exp(-A_r\bar{\phi}_r^{1/2})\right\}; \quad V < 0 \end{aligned}\right\} \tag{1}$$

$$V(t) = V_b + v(t)\cos \omega t \tag{2}$$

$$I_{rect}(t) = \int_{-\pi}^{\pi} I[V_b + v(t)\cos \theta]d\theta/2\pi \tag{3}$$

$$\begin{aligned} I_{rect}(t) \cong\ & J_i \exp(-A_{ib}\bar{\phi}_{ib}^{1/2})\left\{\bar{\phi}_{ib}[I_o(z_i v) - 1] - \beta_{ib} v I_1(z_i v)\right\} \\ & -J_i \exp(-A_{ib}\bar{\phi}'^{1/2}_{ib})\left\{\bar{\phi}'_{ib}[I_o(z'_i v) - 1] - \beta_{ib} v I_1(z'_i v)\right\} \end{aligned} \tag{4}$$

$$z_i = \beta_{ib} A_{ib} (4\bar{\phi}_{ib})^{-1/2}$$

Figure 3.– Outline of the derivation of the rectified current I_{rect}. $\bar{\phi}_r$ is analogous to $\bar{\phi}_f$ but with the 1 and 2 interchanged. Similarly with $A_r \cdot J_r = -J_f \cdot s_1$ and s_2 are the turning points for an electron of energy E_{F_1} and x is measured from metal 1 for the reverse (r) biased case ($V < 0$).

In the expression for $I_{rect}(t)$, i is chosen as either f or r for $V > 0$ or $V < 0$, respectively. The subscript b refers to parameters evaluated at the bias voltage V_B. z_i' is the same as z_i with β_{ib} replaced by $1 - \beta_{ib}$. Similarly for $\bar{\phi}_{i'b}$.

I_0 and I_1 are the zero and first order Bessel functions which describe the curvature characteristics of the rectified signal.

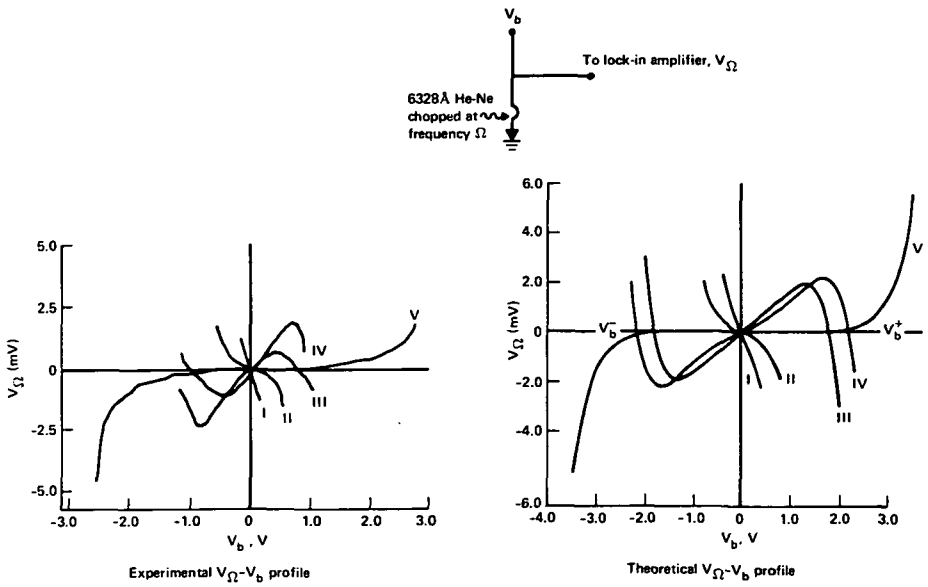

Figure 4.– Rectification experiments with He-Ne 6328 Å radiation. Experimental results are shown on the left-hand side; the theoretical comparison on the right-hand side. V_Ω is the phase sensitively detected signal at the chopping frequency of 1 kHz. V_B is the voltage bias.

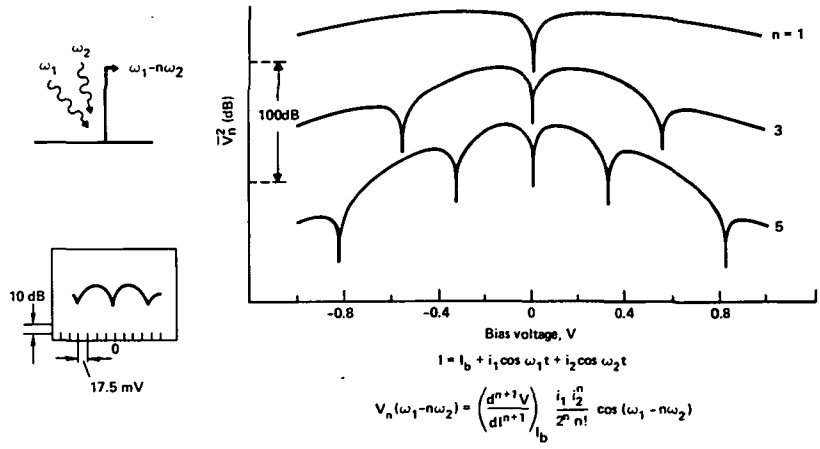

Figure 5.– Current dependent nonlinear mixing processes in metal-metal-barrier-metal structures. I_b is the current bias; $i_1 \cos \omega_1 t$ and $i_2 \cos \omega_2 t$; currents induced by two incident laser signals at frequency ω_1 and ω_2 respectively. $\overline{V_n^2}$ is the mean square i.f. signal at frequency $\omega_1 - n\omega_2$. The insert shows an experimental curve obtained by Evensen and Sakuma in the sub-millimeter range for $n = 5$. Figure 5 shows curves for $n = 1, 3, 5$.

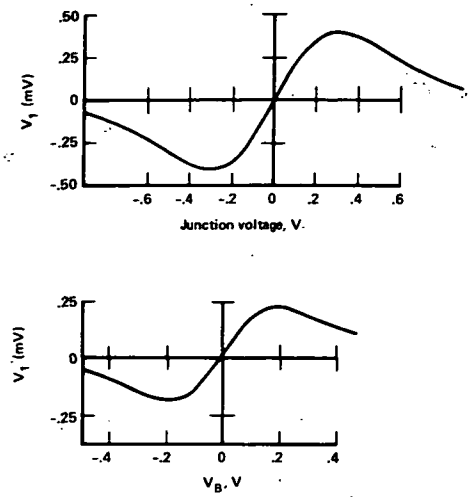

Figure 6.– Current rectification at 1.15 μ. The top curve shows V_1 (V_n for n = 1) and the bottom curve the theoretical comparison for suitably chosen parameters (ref. 1).

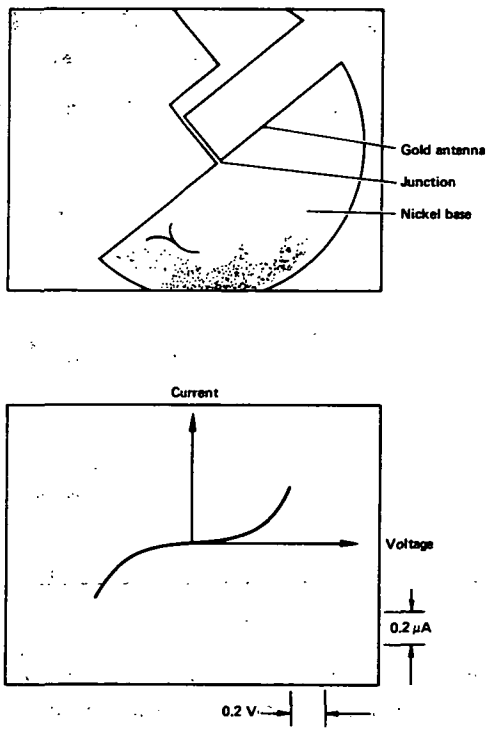

Figure 7.– Photolithographically fabricated metal-barrier-metal structure and associated antenna coupler. The lower curve displays the experimentally measured current-voltage characteristic. The structure is planar, the black background being the nonabsorbing silicon substrate.

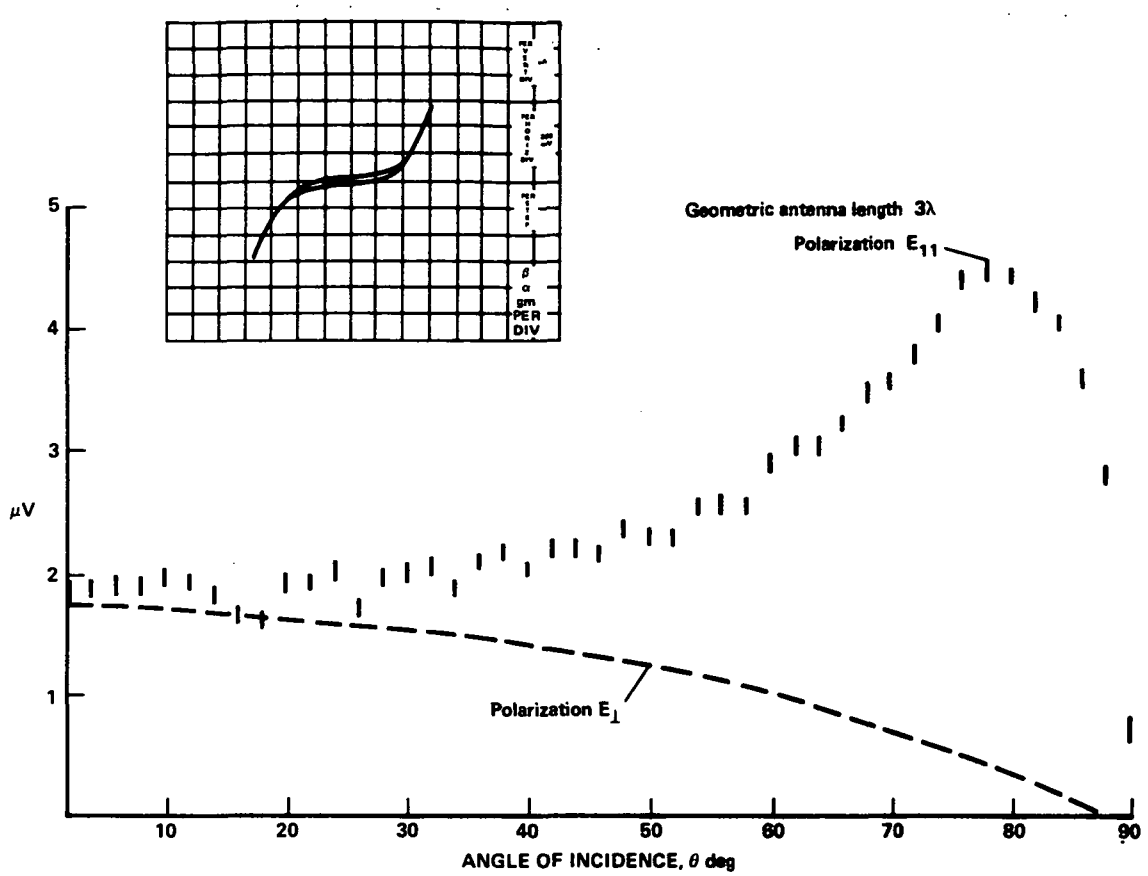

(a) The E_{11} signal displays antenna coupling, the $E_{\perp}$ signal a thermally induced signal.

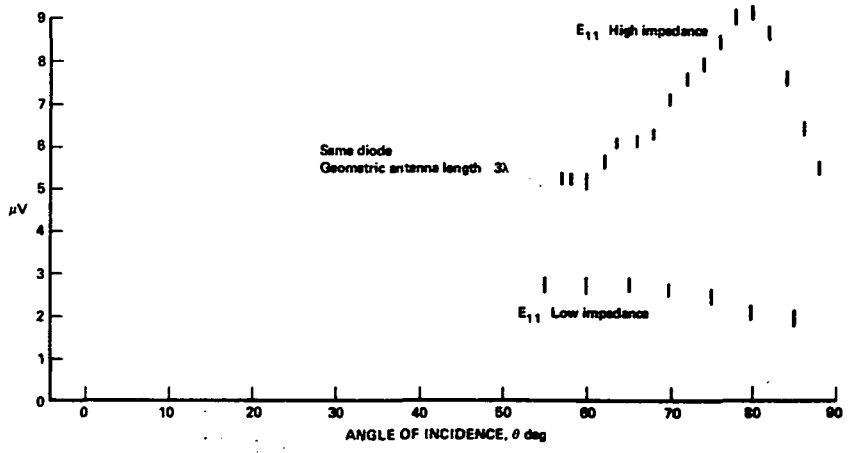

(b) High impedance junction (same one as for fig. (8a)) for E_{11} induced signal displays antenna coupling. A short circuit junction (lower curve) shows only the thermal response for E_{11} as well as for $E_{\perp}$.

Figure 8.– Antenna coupling and rectification with the evaporated structure of figure 7. The induced rectified voltages are due to 10.6 μm, 10 W/cm^2 of CO_2 laser beam intensity. The beam is directed in the plane containing the diode and normal to the substrate surface and θ is the angle of the propagation vector with respect to the normal. E_{11} represents the electric field polarized along the gold wire and $E_{\perp}$, polarized perpendicularly.

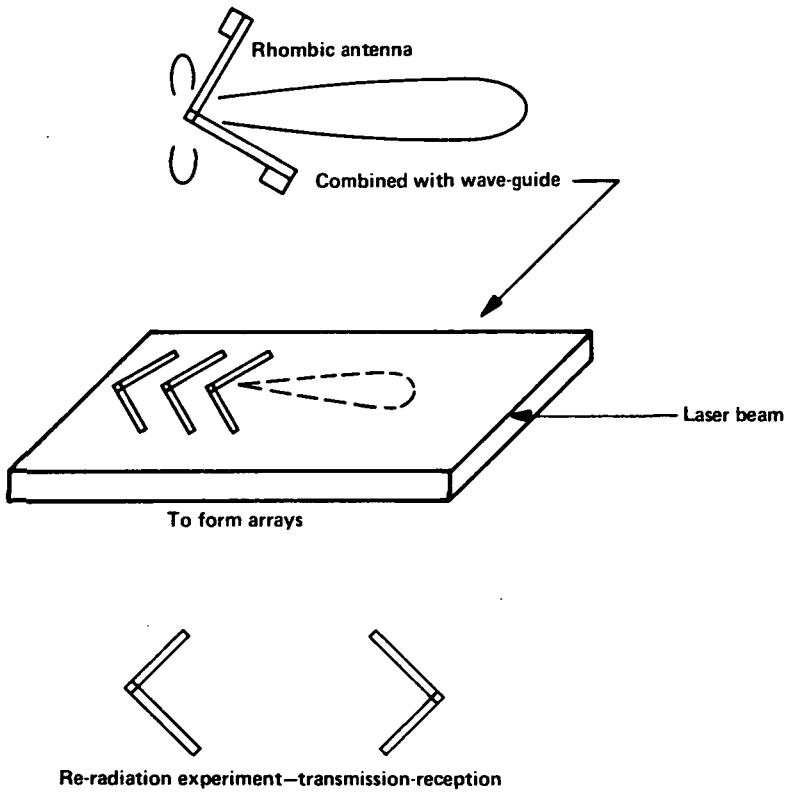

Figure 9.– Proposed work using evaporated antenna structures.

DISCUSSION

Max Garbuny, Westinghouse – The cross section of an antenna or atom is of the order of $\lambda^2/2\pi$. Do these junctions exhibit this same cross section?

Ken Gustafson: The $\lambda^2/2\pi$ is appropriate for a dipole antenna. Since our diodes exhibit many lobes, they are no simple dipoles. So the antenna area will depend upon this lobe structure.

Ali Javan: We find that one can characterize the area by something like λ^2; it turns out that for a 10-μ junction it is approximately $(20\,\mu)^2$.

Katasonori Shimada, J. P. L. – The volt-ampere characteristics you show always have a symmetric shape. If you use different metals for example, gold and nickel, could you get a true diode characteristic?

Ken Gustafson: We are looking at that whole question of whether its possible to obtain an asymmetric VI characteristic. It's too early to tell. The problem is that as you examine the theory, the odd order or rectification coefficients come in as the difference between the work functions of the metals. The other coefficients come in as the sum. So to get the characteristic you ask for, we need to use metals with large work function difference. An interesting question is: could this converter be as good as a thermoelectric converter, because the thermionic converter suffers from precisely the same fault – that is, the thermoelectric voltage is proportional to the difference between the two work functions.

Ali Javan, M. I. T.: A comment. If you keep making and breaking a point contact diode, looking for its characteristics with various pressures, or oxide thicknesses, you are able to get occasional asymmetric characteristics. But with our evaporated junctions, they are always symmetrical.

Ken Gustafson: Yes, we have found the same.